MJFAS
Malaysian Journal of Fundamental and Applied Sciences

R. X. P. Lam et al. | Malaysian Journal of Fundamental and Applied Sciences, Vol. 22 (2026) 903-916

RESEARCH ARTICLE

Anti-Inflammatory Potential of *Momordica charantia* through Integrative Network Pharmacology and Molecular Docking Analysis

Renee Xuan Pin Lam[a], Hong-Yeng Leong[b], Muhammad Helmi Nadri[b], Kian-Kai Cheng[a,*]

[a]Faculty of Chemical & Energy Engineering, Universiti Teknologi Malaysia, Johor, Malaysia, [b]Faculty of Science, Universiti Teknologi Malaysia, Johor, Malaysia

Abstract Recent studies have demonstrated the therapeutic potential of *Momordica charantia* (bitter gourd) against inflammation. However, the specific biological targets and molecular mechanisms underlying these effects remain to be fully elucidated. This study aimed to characterize the anti-inflammatory potential of bioactive compounds from *Momordica charantia*. Specifically, the objectives were to: (i) evaluate the drug-likeness and ADMET (absorption, distribution, metabolism, excretion, and toxicity) profiles of its bioactive constituents, (ii) map multi-target regulatory network through network pharmacology, and (iii) analyze binding interactions with key inflammatory targets using molecular docking. An integrative computational framework combining Lipinski's Rule of Five assessment, ADMET profiling, network pharmacology, and molecular docking was employed. Eight major bioactives were analyzed: beta-sitosterol glucoside (BSG), stigmasterol glucoside (SG), trigonelline, galactonic acid, gamma-aminobutyric acid (GABA), isoleucine, leucine, and valine. All eight selected *M. charantia* bioactive compounds adhere to Lipinski's Rule of Five and were predicted to be non-toxic, except for trigonelline, which exhibited moderate toxicity. Subsequent network pharmacology analysis identified 28 potential therapeutic targets associated with inflammation, from which five core targets, alongside the closely associated receptor IGF1R, were prioritized for molecular docking analysis. Molecular docking revealed that the charantin metabolites, BSG and SG, exhibited higher predicted multi-target binding affinities compared to other constituents. Notably, SG displayed exceptional affinity for IGF1R (−10.9 kcal/mol) and EGFR (−10.2 kcal/mol), while BSG showed strong interaction with NOS3 (−10.5 kcal/mol) and PPARG (−8.8 kcal/mol). Mechanistically, the compounds are predicted to modulate the PI3K–Akt signaling axis via key targets (IGF1, EGFR, NOS3, HSP90AA1), while concurrently influencing the IL-17, HIF-1, and FoxO signaling pathways to suppress inflammation. This study identifies beta-sitosterol glucoside and stigmasterol glucoside as potential multi-target modulators of inflammatory pathways, which warrant subsequent experimental validation to confirm clinical efficacy. Taken together, these findings provide structural insights into the anti-inflammatory properties of *M. charantia* and support its potential as a source of natural therapeutic agents.

***For correspondence:**
chengkiankai@utm.my

Received: 04 May 2026
Accepted: 21 May 2026

© Copyright R. X. P. Lam. This article is distributed under the terms of the Creative Commons Attribution License, which permits unrestricted use and redistribution provided that the original author and source are credited.

Keywords: *Momordica charantia*, Inflammation, Type 2 Diabetes Mellitus, Network pharmacology, Molecular docking.

Introduction

Inflammation is a fundamental immune response to harmful stimuli, such as pathogens, tissue injury, or toxic compounds [1]. In recent years, chronic inflammation has been increasingly implicated in the pathogenesis of various diseases, including cardiovascular disease, type 2 diabetes, cancer, neurological disorders, and arthritis [2]. Although conventional therapeutics, particularly nonsteroidal

anti-inflammatory drugs (NSAIDs) and corticosteroids, are widely utilized for their potent efficacy, their long-term application is often limited by significant adverse side effects.

Momordica charantia (bitter gourd) is well-established for its hypoglycemic activity [3], [4], [5]. More recently, research has demonstrated that both *M. charantia* and its key bioactive compound, charantin, suppress the expression of pro-inflammatory mediators (including IL-6, TNF-α, IL-1β, COX-2, and iNOS) while modulating IL-10 expression in lipopolysaccharide-treated murine macrophages [6]. Furthermore, studies from Yang *et al*. showed that *M. charantia* exerts anti-inflammatory effects by inhibiting TAK1, thereby blocking NF-κB and Activator Protein-1 (AP-1) activation in macrophages [7]. These findings are supported *in vivo*, where supplementation significantly reduced pro-inflammatory markers (including nitric oxide, aspartate aminotransferase, alanine aminotransferase, and C-reactive protein) and organ damage while upregulating IL-10 in mice [8]. Similarly, Liaw *et al*. [9] reported that an ethanol extract from wild *M. charantia* vines exerts anti-inflammatory properties by inhibiting nitric oxide (NO) production, aligning with the findings of Chao *et al*. [8]. However, the precise molecular targets driving these therapeutic effects remain inadequately characterized.

To address this gap, this study systematically investigates the multi-target anti-inflammatory mechanisms of diverse *M. charantia* bioactive compounds, including steroidal glucosides, alkaloids, and amino acids. We integrate network pharmacology with molecular docking to provide a comprehensive understanding of their interactions with key targets and pathways. Network pharmacology is used to map complex compound–target–pathway interactions to reveal the role of these bioactives in disease regulation, while molecular docking provides structural insights into binding affinities and ligand conformations at specific target sites. Collectively, these approaches establish a robust framework for identifying promising anti-inflammatory lead compounds from *M. charantia*.

Materials and Methods

Drug-likeness and Pharmacokinetics of Selected Bioactive Compounds

Eight candidates for *M. charantia* metabolites were selected based on literature and internal metabolomics data. These included the two primary steroidal glucosides constituting charantin, namely beta-sitosterol glucoside (BSG) and stigmasterol glucoside (SG), alongside trigonelline, galactonic acid, gamma-aminobutyric acid (GABA), isoleucine, leucine, and valine. The drug-likeness and pharmacokinetic properties of these compounds were predicted using the ADMETlab (https://admetlab3.scbdd.com) and SwissADME (http://www.swissadme.ch) web servers [10]. Adherence to Lipinski's Rule of Five was evaluated based on four key parameters: molecular weight ≤ 500 Da, lipophilicity (MLOGP) ≤ 4.15, hydrogen bond donors (NH or OH) ≤ 5, and hydrogen bond acceptors (N or O) ≤ 10. Additionally, toxicity profiles were assessed using the ProTox-II server (https://tox-new.charite.de/protox_II) [11].

Identification of Potential Bioactive Targets and Inflammation-Related Genes

The chemical structures of the selected *M. charantia* bioactive compounds were retrieved from the PubChem database (https://pubchem.ncbi.nlm.nih.gov/) in both Structure-Data File (.sdf) and canonical SMILES formats. Putative protein targets for these compounds were predicted using the PharmMapper (https://www.lilab-ecust.cn/pharmmapper/) [12], [13] and SwissTargetPrediction (http://www.swisstargetprediction.ch/) [14], [15] web servers. For PharmMapper, the analysis was restricted to *Homo sapiens* targets, and results were filtered using a Normalized Fit Score threshold of ≥ 0.6 [16]. For SwissTargetPrediction, targets were retained only if they met a probability threshold of $P > 0.4$ [17], [18]. Concurrently, inflammation-related target genes were mined from the GeneCards V5.18 (https://www.genecards.org/) [19] and DisGeNET 7.0 (https://www.disgenet.org/) [20], [21] databases. Finally, the intersection between the *M. charantia* compound targets and the inflammation-related genes was identified using an online Venn diagram tool (https://bioinformatics.psb.ugent.be/webtools/Venn/) to pinpoint potential therapeutic targets for subsequent analysis.

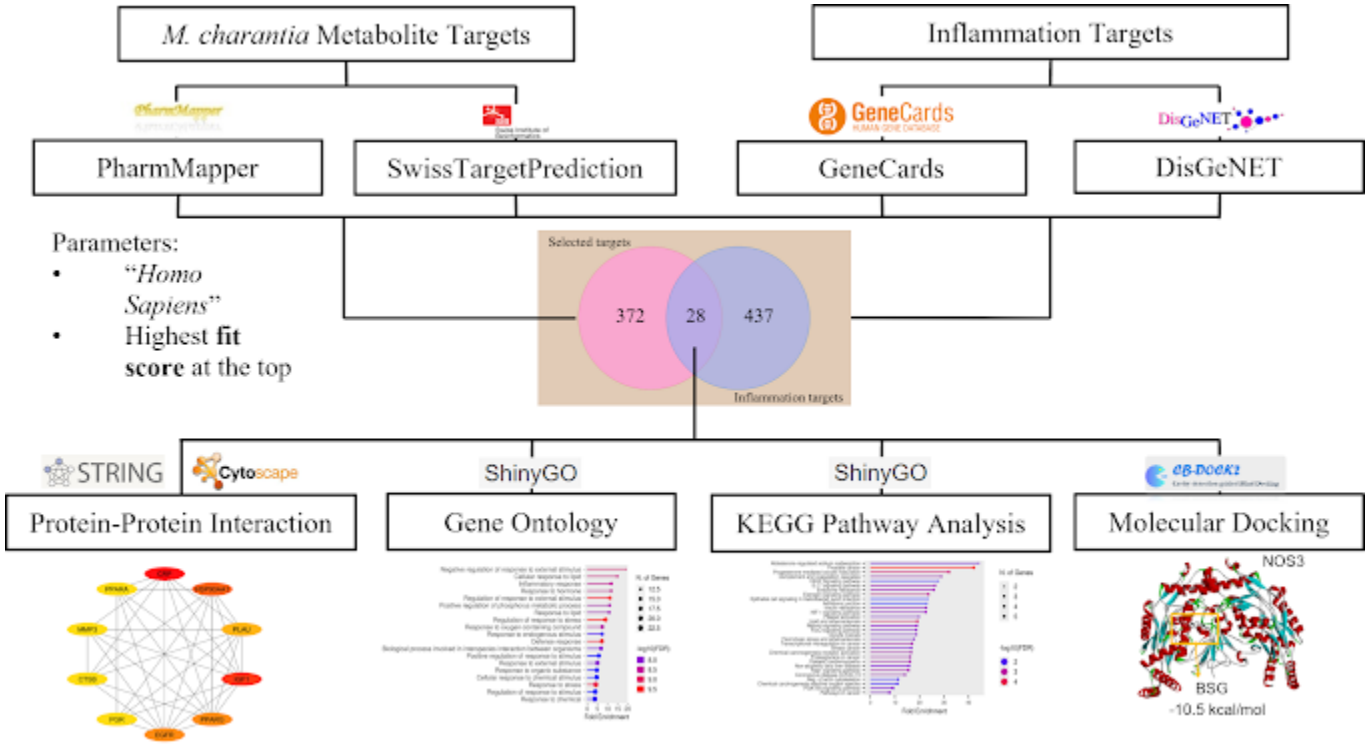


Figure 1. Workflow for the computational study of network pharmacology and molecular docking

Construction of PPI network

The overlapping target genes were mapped to a Protein–Protein Interaction (PPI) network using the STRING database (https://string-db.org/) [22], with the organism restricted to *Homo sapiens* and a minimum interaction confidence score of ≥ 0.4 [16], [17]. This score represents the database's standard 'medium confidence' threshold, chosen to capture a comprehensive functional interactome without introducing excessive computational noise. The resulting network was visualized using Cytoscape software. To identify core regulatory genes (hubs), topological analysis was performed using the CytoHubba plugin based on Degree centrality ranking [23]. Furthermore, densely connected functional modules were detected using the Molecular Complex Detection (MCODE) plugin [24], [25] with the following parameters: degree cutoff = 2, node score cutoff = 0.2, K-core = 2, and maximum depth = 100 [26]. Finally, the identified core targets were annotated with standard gene symbols using the UniProtKB database (https://www.uniprot.org/) [27].

Gene Ontology (GO) and KEGG Pathway Enrichment Analysis

To elucidate the biological functions and signaling pathways associated with the identified targets, Gene Ontology (GO) enrichment and Kyoto Encyclopedia of Genes and Genomes (KEGG) pathway analyses were performed using ShinyGO 0.82 (http://bioinformatics.sdstate.edu/go/). The GO analysis encompassed three primary categories: Biological Process (BP), Cellular Component (CC), and Molecular Function (MF). For all enrichment analyses, the species was restricted to *Homo sapiens*, and pathways were considered statistically significant if the adjusted *p*-value (FDR) was < 0.05.

Molecular Docking Simulation

The crystallographic structures of the identified core targets were retrieved from the RCSB Protein Data Bank (https://www.rcsb.org/) in .pdb format. The specific structures utilized were: NOS3 (PDB ID: 1M9R), HSP90AA1 (PDB ID: 8AGI), EGFR (PDB ID: 3W32), PTPN1 (PDB ID: 2QBP), PPARG (PDB ID: 7AWD), and IGF1R (PDB ID: 3LVP). Corresponding ligand structures were obtained from PubChem in .sdf format. Molecular docking was performed using the CB-Dock2 server (https://cadd.labshare.cn/cb-dock2/) which employs a cavity-detection guided blind docking approach [28]. Protein and ligand files were uploaded directly, and docking was executed using default parameters. The resulting ligand–protein complexes were saved in .pdb format. Finally, the binding poses and specific molecular

interactions (hydrogen bonds, hydrophobic contacts) were visualized and analyzed using BIOVIA Discovery Studio Visualizer.

Results and Discussion

Oral Bioavailability and Pharmacokinetics of *M. charantia* Bioactives

The drug-likeness of the selected *M. charantia* bioactive compounds was evaluated using Lipinski's Rule of Five (Ro5), with results summarized in Table 1 (full analysis in Supplementary Table S1). All eight compounds satisfied the criteria for oral drug-likeness. Specifically, trigonelline, GABA, and the branched-chain amino acids (BCAAs) demonstrated strict compliance with no violations. Meanwhile, beta-sitosterol glucoside (BSG), stigmasterol glucoside (SG), and galactonic acid each exhibited a single violation. As the rule permits up to one violation, these results suggest that all selected bioactives possess the necessary physicochemical properties to be developed as orally active therapeutics.

Table 1. Lipinski Rules of Five analysis and oral toxicity profiles of selected *Momordica charantia* bioactive compounds. MW: Molecular weight (Toxicity Class 1-3: toxic, lethal if consumed; Class 4-5: moderate toxicity, harmful if consumed; Class 6: non-toxic).

No.	Compound	Compliance with Lipinski's Rule of 5 (Rejected if > 1 violation)	Predicted LD50 (mg/kg)	Predicted Toxicity Class
1	Beta-sitosterol glucoside (BSG)	Yes; 1 violation: MW>500	8000	6
2	Stigmasterol glucoside (SG)	Yes; 1 violation: MW>500	8000	6
3	Trigonelline	Yes; 0 violation	3720	5
4	Galactonic Acid	Yes; 1 violation: NH or OH>5	9100	6
5	Gamma-aminobutyric acid (GABA)	Yes; 0 violation	12680	6
6	Isoleucine	Yes; 0 violation	10000	6
7	Leucine	Yes; 0 violation	10000	6
8	Valine	Yes; 0 violation	12680	6

The ADME profiles of the bioactive compounds were systematically evaluated, with detailed pharmacokinetic parameters summarized in Supplementary Table S2. Specifically, the analysis focused on Caco-2 permeability, Human Intestinal Absorption (HIA), and oral bioavailability thresholds (F20, F30). Caco-2 predictions indicated moderate permeability across the dataset, with values ranging from −5.34 log cm/s (GABA; highest) to −5.94 log cm/s (stigmasterol glucoside; lowest). While human intestinal absorption (HIA) is predicted to be high (category 0) for all compounds, the Caco-2 scores indicate only moderate cellular permeability, suggesting potential pharmacokinetic limitations that must be addressed in future drug formulation efforts. Furthermore, every compound demonstrated favorable oral bioavailability, exceeding the benchmarks of 20% and 30% bioavailability.

Distribution analysis (Supplementary Table S2) revealed that while most compounds possess optimal plasma protein binding (<90%), stigmasterol glucoside showed extensive binding (98.52%), which could impact its bioavailability. All compounds demonstrated favorable Volume of Distribution (0.04–20 L/kg). However, a critical re-evaluation of the Blood–Brain Barrier (BBB) predictions indicates that while some smaller metabolites may cross the BBB, the permeability of larger steroidal glucosides is likely restricted, necessitating cautious interpretation. Regarding metabolic stability, none of the compounds inhibited the five major cytochrome P450 isoenzymes (CYP1A2, CYP2C19, CYP2C9, CYP2D6, and CYP3A4), suggesting a low risk of metabolic drug–drug interactions or toxicity [29], [30]. Finally, elimination profiling revealed distinct patterns: beta-sitosterol glucoside, stigmasterol glucoside, trigonelline, and galactonic acid were predicted to have low plasma clearance, where the volume of plasma that contains drug or metabolic waste to be entirely cleared by kidneys or liver per unit time were calculated [31]. Whereas the remaining compounds exhibited moderate clearance. Correspondingly, half-life predictions indicated rapid elimination from plasma for leucine and valine, while other compounds demonstrated intermediate half-lives.

The oral toxicity profiles of the compounds were predicted using the ProTox-II server, with results detailed in Table 1. The analysis classified most of the bioactive compounds (including BSG, SG, galactonic acid, GABA, and BCAAs) as Class 6 (Non-toxic), with predicted LD50 values ranging from

8000 mg/kg to 12,680 mg/kg. In contrast, Trigonelline fell into Class 5 (LD50 = 3720 mg/kg), warranting slightly more cautious dosing considerations. Taken together, the combination of favorable oral bioavailability, optimal distribution, and minimal toxicity risk positions these *M. charantia* constituents as promising candidates for clinical translation.

Identification of Potential Therapeutic Targets

The molecular targets of the selected *M. charantia* bioactive compounds were predicted using two complementary tools: PharmMapper (Normalized Fit Score ≥ 0.6) and SwissTargetPrediction (Probability > 0.4). These operational cutoffs were explicitly selected to filter out low-probability targets while preserving a sufficient dataset for robust network construction. In parallel, inflammation-related targets were curated from the GeneCards (16,356 targets) and DisGeNET (467 targets) databases. To ensure the reliability of the disease-associated gene set, only targets present in both databases were retained. Subsequently, the predicted compound targets were intersected with this refined inflammation gene set. This analysis identified 28 overlapping targets representing the potential therapeutic mechanism of *M. charantia* against inflammation (Table 2, Supplementary Figure S1). To evaluate prediction reliability, these targets were cross-referenced with existing literature to validate their roles in mediating anti-inflammatory bioactivities (Supplementary Table S3). Finally, the validated target set was imported into Cytoscape for network construction and topological analysis. The identified targets orchestrate a range of biological functions, including the modulation of inflammatory mediators like NOS3 and MMP3, as well as the activation of signaling receptors such as EGFR and PPARG. This breadth of activity highlights the multi-target potential of *M. charantia* in treating inflammation.

Table 2. Potential therapeutic targets associated with bioactive compounds of *Momordica charantia* and inflammation.

Bioactive compounds of *Momordica charantia*	Potential gene targets associated with inflammation
BSG, GABA, Isoleucine, Leucine, SG, Valine	NOS3
BSG, Isoleucine, Leucine, SG, Valine	F2
Galactonic acid, Isoleucine, Leucine, SG, Valine	HSP90AA1
BSG, Galactonic acid, Isoleucine, SG	EGFR
BSG, Galactonic acid, Leucine, SG	PTPN1
BSG, Isoleucine, Leucine, SG	MMP3
Isoleucine, Leucine, Trigonelline, Valine	PRDX5
BSG, Galactonic acid, SG	APCS, ANG, CTSB
BSG, Isoleucine, SG	MAPK14
BSG, Isoleucine, Leucine	MIF
BSG, SG	PGR, STS, NR1H4, NR3C2, PPARG, ITGAL
Isoleucine, Valine	F7
BSG	PPARA
SG	IGF1, PDE5A, PARP1
Galactonic acid	LTF, TREM1, PLAU, FCAR
GABA	CRP

Protein-protein Interactions: Network of *M. charantia* Associated with Inflammatory Targets

To elucidate the functional connectivity among the identified targets, a Protein-Protein Interaction (PPI) network was constructed using the STRING database and visualized in Cytoscape (Figure 2). The resulting network comprised 28 nodes and 91 edges, with an average node degree of 6.5 (PPI enrichment p < 1.0e-16). While most of the network was highly interconnected, STS and PRDX5 appeared as disconnected nodes. Overall, this dense connectivity suggests that the identified targets do not function in isolation but rather form a cohesive regulatory module, likely coordinating shared inflammatory pathways.

Topological analysis was conducted using the CytoHubba plugin to identify core regulatory targets [23]. The top ten targets, ranked by degree score, were identified as: CRP, IGF1, HSP90AA1, PPARG, EGFR, PLAU, PPARA, CTSB, PGR, and MMP3. In the network visualization (Figure 3), node colour represents ranking importance, transitioning from red (high degree) to yellow (lower degree). Complementary analysis using the MCODE plugin detected a significant functional cluster (Figure 4) containing 12 nodes and 41 edges, indicative of a highly interconnected protein module. This cluster, seeded by IGF1, includes key inflammatory mediators such as HSP90AA1, CTSB, PGR, PARP1, MMP3, PTPN1, CRP, PLAU, MAPK14, PPARA, and PPARG. The results suggested that *M. charantia* bioactives likely modulate inflammation by simultaneously targeting this specific protein complex.

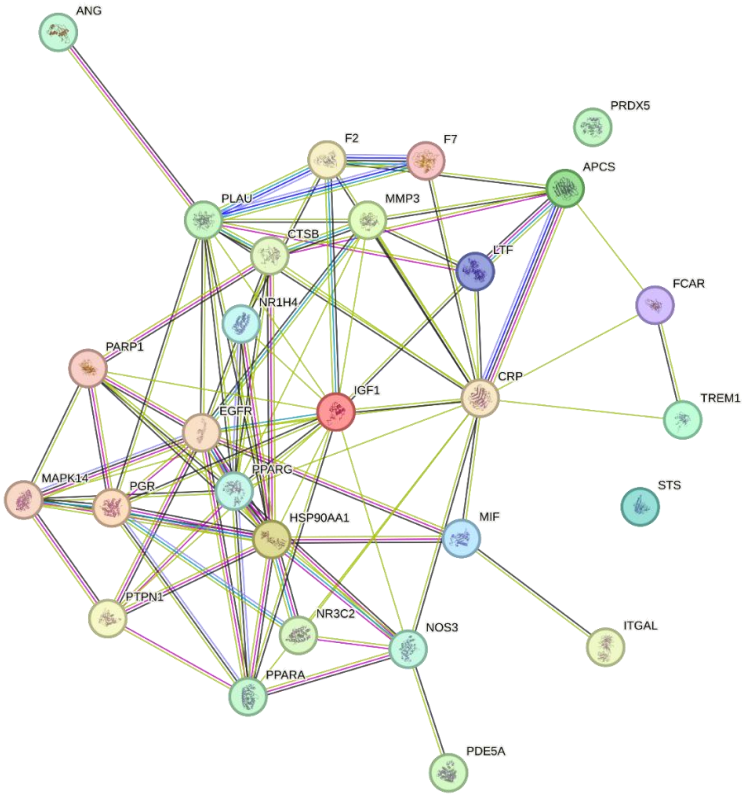


Figure 2. PPI Network Construction. Interaction map of the 28 identified targets associated with *M. charantia* and inflammation. The network exhibits significant interconnectivity (Nodes: 28; Edges: 91; Average Node Degree: 6.5; PPI Enrichment p < 1.0e-16).

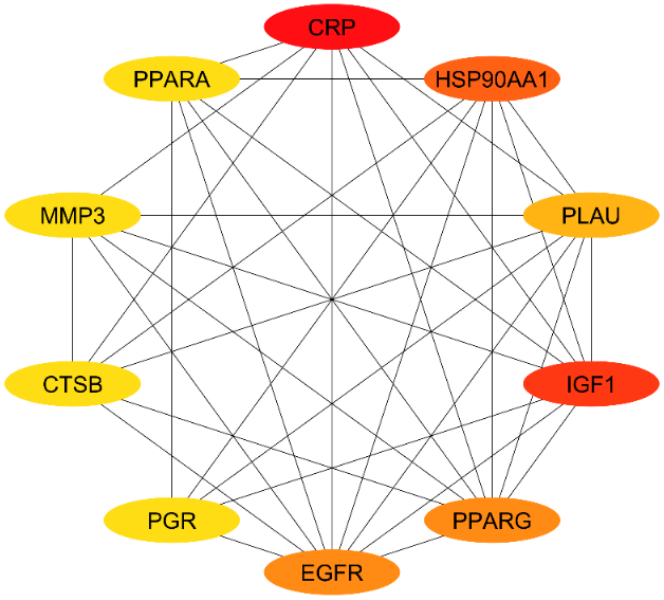


Figure 3. Top 10 genes identified using the CytoHubba plugin in Cytoscape to highlight core regulatory targets. (Yellow to red for higher ranking)

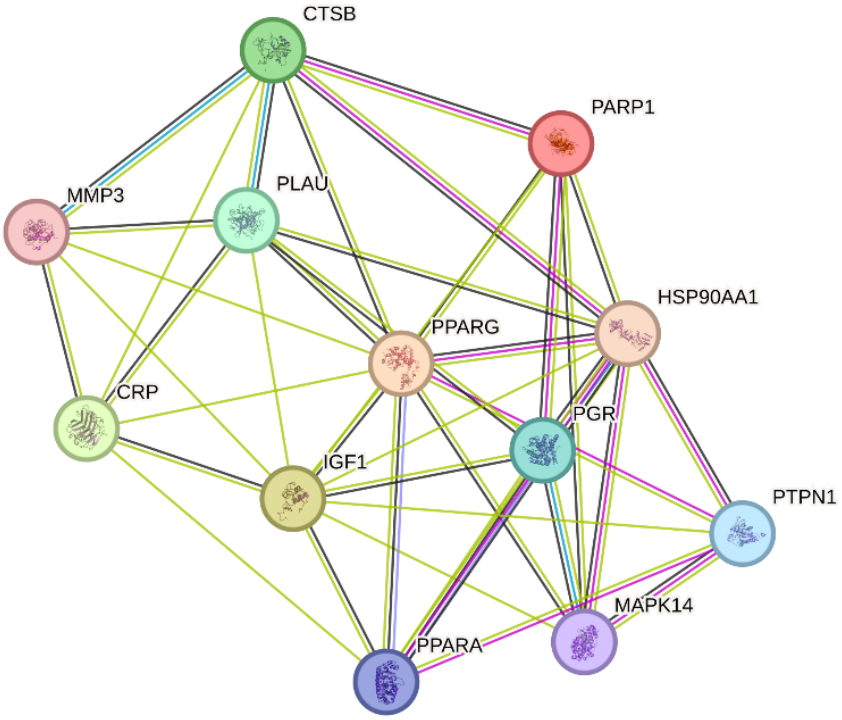


Figure 4. MCODE Cluster Analysis. Visualization of the top-ranking cluster seeded by IGF1 (12 nodes, 41 edges). The module highlights a dense interaction network involving critical therapeutic targets.

GO and KEGG Pathway Enrichment Analysis

Functional enrichment analysis via ShinyGO 0.82 (Figure 5) provided mechanistic insights into the anti-inflammatory effects of the selected compounds. In terms of Biological Processes, the targets were heavily involved in regulating inflammatory and defense responses to external stimuli. Cellular Component analysis indicated that these proteins predominantly operate within the extracellular matrix and vesicle systems (secretory, cytoplasmic, and intracellular). Furthermore, Molecular Function data revealed that the bioactives likely exert their effects by modulating nuclear receptor activity and signaling receptor binding.

KEGG pathway enrichment analysis (Figure 6) revealed that the target genes are involved in multiple inflammation-associated signaling cascades. Significant enrichment was observed for the IL-17 signaling pathway (hsa04657), HIF-1 signaling (hsa04066), and FoxO signaling (hsa04068), as well as metabolic and disease-related pathways such as insulin resistance (hsa04931), diabetic cardiomyopathy (hsa05415), and pathways in cancer (hsa05200). A primary focal point was the PI3K–Akt signaling pathway (hsa04151), a well-established regulator of systemic inflammation and macrophage polarization [32]. Our data indicates that *M. charantia* bioactives are likely modulate this pathway via interactions with IGF1, EGFR, NOS3, and HSP90AA1 (Supplementary Figure S2), thereby attenuating NF-κB activity and cytokine release. To further investigate this potential, molecular docking simulations were performed to evaluate the binding strength between the selected bioactives and these core inflammatory targets.

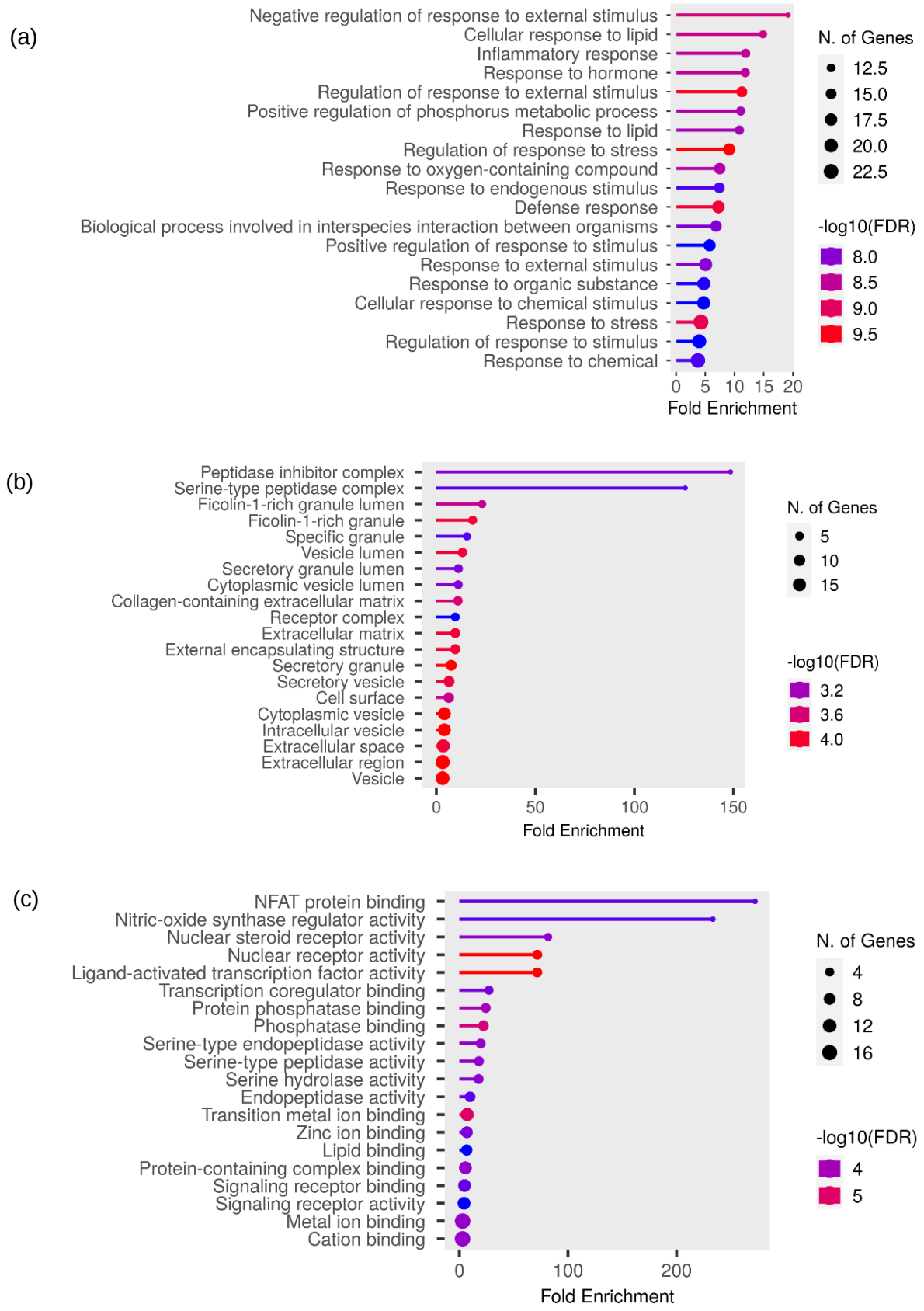


Figure 5. GO functional enrichment analysis from 28 targets of *Momordica charantia* against inflammation: (a) Biological processes; (b) Cellular components; (c) Molecular functions.

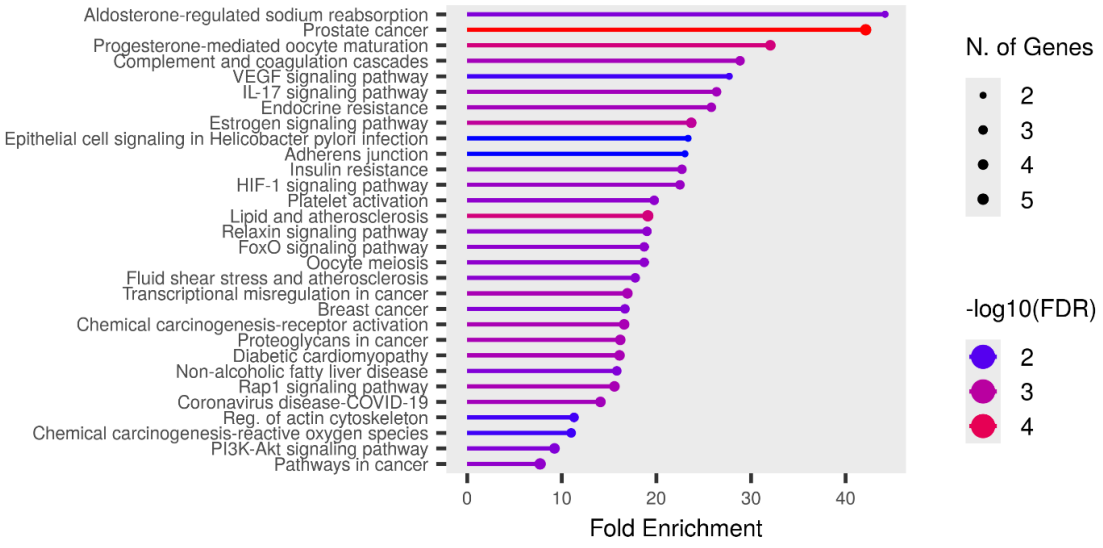


Figure 6. KEGG functional enrichment analysis from 28 targets of *Momordica charantia* against inflammation

Compound-Target-Pathway Network Analysis

We constructed a compound–target–pathway (C–T–P) network to visualize the multi-dimensional interactions of *M. charantia* bioactives (Figure 7). The network topology reveals that each compound is linked to numerous targets, which subsequently map to critical inflammation-related pathways (e.g., FoxO, HIF-1, IL-17). This high degree of connectivity underscores a synergistic therapeutic potential, suggesting that its anti-inflammatory power stems from the synergistic regulation of a broad signaling network rather than the inhibition of a single protein.

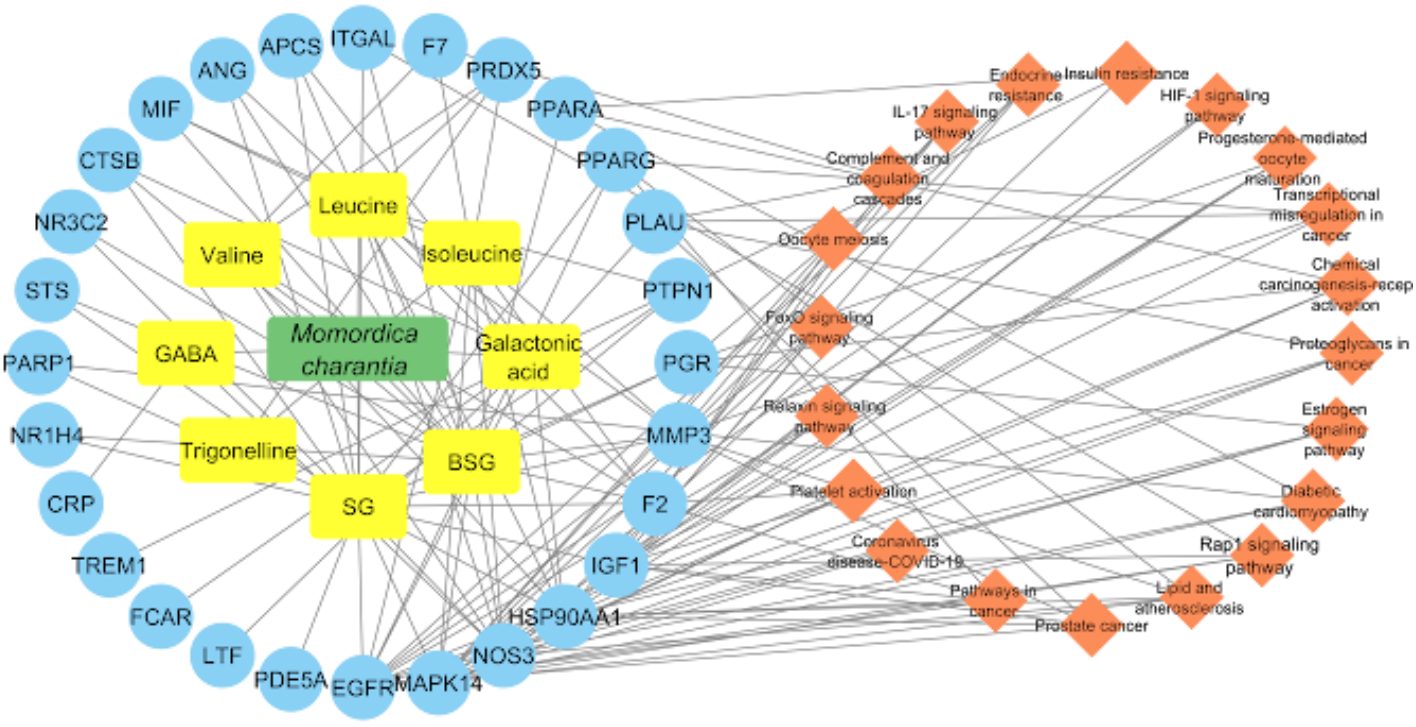


Figure 7. Compound-Target-Pathway analysis of *M. charantia* constructed by the STRING database and Cytoscape 3.7.2. Yellow: *M. charantia* bioactives; Blue: therapeutic targets; Orange: Pathways.

Network pharmacology has been adopted and widely used in the study of elucidating the multi-target anti-inflammatory mechanisms of plant-derived phytochemicals. Among the most extensively studied phytochemicals using this approach is quercetin, which has been demonstrated to exert anti-inflammatory effects through the NF-κB and MAPK signaling pathways. Molecular docking studies have confirmed its stable binding interactions with core inflammatory targets including AKT1, TNF, and IL-6 [33]. Similarly, curcumin, a polyphenol derived from *Curcuma longa*, was reported to engage 135 potential anti-inflammatory targets across the TNF, HIF-1, PI3K-Akt, JAK-STAT, and MAPK signaling pathways. This was established through an integrated network pharmacology, molecular docking, and molecular dynamics simulation approach, with in vitro validation confirming the suppression of IL-1β, IL-6, and TNF in LPS-induced RAW 264.7 macrophages [34].

Furthermore, the natural flavonoid kaempferol was shown to modulate TNF, IL-17, NF-κB, PI3K-Akt, and MAPK pathways, identifying MAPK8, PPARγ, and NF-κB as core anti-inflammatory targets [35], [36]. Moreover, berberine, an isoquinoline alkaloid, has been shown to exert strong anti-inflammatory and neuroprotective properties by targeting AKT1, HSP90AA1, SRC, HRAS, IGF1, ALB, EGFR, and CASP3 [37], [38]. The identification of HSP90AA1, EGFR, and IGF1 as primary targets for berberine closely mirrors the core regulatory network identified in our study.

In this context, our findings show that the *M. charantia* bioactives, BSG and SG, may act on the same key pathways (including NF-κB, MAPK, and PI3K-Akt) as these established plant-based agents. Furthermore, coupled with their favorable oral bioavailability, optimal distribution, and minimal toxicity risks, these charantin constituents may offer robust pathway engagement comparable to standard phytochemicals. To further evaluate this theoretical efficacy and provide structural insights into these specific target engagements, molecular docking simulations were subsequently performed.

Molecular Docking of Potential Gene Targets

Molecular docking simulations were performed to elucidate the binding affinity and molecular interactions between *M. charantia* bioactive compounds and the selected protein targets. Five core targets from the 28 overlapping targets (NOS3, HSP90AA1, EGFR, PTPN1, and PPARG), alongside the closely associated receptor IGF1R, were prioritized for molecular docking. The selection is based on high degree centrality in the PPI network or presence within the core MCODE functional cluster, together with well-established biological relevance in mediating inflammatory pathways. Although IGF1 emerged as a core regulatory hub, we prioritized its cognate receptor, IGF1R, for molecular docking because targeting the receptor is a more reliable strategy for blocking downstream inflammatory cascades [45, 60, 61, 62]. Consequently, IGF1R serves as a much more direct and robust structural endpoint for evaluating the anti-inflammatory potential of *M. charantia* bioactives. The binding affinities of the bioactive compounds for the selected targets were compared with standard reference ligands, which were selected for each target based on clinical relevance or their known experimental inhibitory activity against the respective proteins. The stability of the ligand-protein complex was evaluated based on binding energy, where more negative values indicate a thermodynamically stronger interaction. The conformation exhibiting the lowest binding energy was selected as the most probable physiological binding pose [39], [40], [41].

The binding affinities of the eight bioactive compounds against six key inflammation-associated targets are summarized in Table 3. Notably, the steroidal glucosides BSG and SG demonstrated superior binding scores compared to standard reference ligands. Specifically, they outperformed L-NIO (targeting NOS3) [42], AG1478 (EGFR) [43], [44], TCS401 (PTPN1) [45], and pioglitazone (PPARG) [46], [47]; SG also outperformed linsitinib (IGF1R) [48], [49], whereas BSG did not. Only geldanamycin, a potent HSP90AA1 inhibitor [50], [51], exceeded both compounds.

NOS3 (Endothelial NOS) is a central regulator of nitric oxide (NO) formation and is essential for maintaining cardiovascular homeostasis through vasodilation [52]. However, aberrant NOS3 signalling caused by enzyme uncoupling or overexpression in inflammatory states is linked to diverse pathologies, including systemic sclerosis [53], vascular disease [54], and non-alcoholic steatohepatitis (NASH) [46]. Genetic polymorphisms in the *NOS3* gene further predispose individuals to hypertension, obesity, and diabetes [52].

Mechanistically, the PI3K/Akt–NOS3 axis serves as a critical signalling hub in inflammation-driven diseases. For instance, Villegas *et al*. [55] reported that NOS3 suppresses immune responses in cancer via the NOTCH1-PI3K/Akt pathway, while Jiang *et al*. [46] highlighted the therapeutic value of targeting the FXR/PXR-PI3K-Akt-NOS3 axis in liver inflammation. Our investigation positions *M. charantia* as a promising source for NOS3 modulators. In comparative docking studies, the charantin constituents BSG and SG demonstrated exceptional binding energies (−10.5 and −10.3 kcal/mol), surpassing the affinity

of the established NOS3 inhibitor L-NIO (−6.2 kcal/mol) [42]. These findings underscore the potential of *M. charantia* to alleviate inflammation-associated diseases.

Other research showed similar results, whereby the components of charantin displayed promising inhibitory potential against EGFR, a receptor implicated in both metabolic disorders and acute inflammatory responses [56], [57]. Molecular docking revealed that SG (−9.2 kcal/mol) and BSG (−8.8 kcal/mol) formed more stable complexes with EGFR than the reference inhibitor AG1478 (−8.4 kcal/mol). This strong affinity is significant given the emerging role of EGFR inhibition in treating inflammation. For instance, targeting the RAGE/EGFR axis has been shown to reduce epithelial dysfunction in IL-33-mediated pathologies [58]. These findings position *M. charantia* bioactives as potent natural alternatives for modulating EGFR activity and mitigate inflammatory responses.

PTPN1, a key regulator of macrophage plasticity, was effectively targeted by *M. charantia* bioactives. SG (−8.5 kcal/mol) and BSG (−7.4 kcal/mol) both exceeded the binding energy of the known inhibitor TCS401 (−7.0 kcal/mol). Biologically, PTPN1 acts as a critical checkpoint in inflammatory signaling, though its role is highly context dependent. While complete loss of PTPN1 can exacerbate mucosal inflammation and drive M1 macrophage polarization [59], its upregulation is frequently observed in malignancies [60]. In the hyperactive states, targeted inhibition of PTPN1 has been shown to shift macrophages toward an anti-inflammatory M2 phenotype [61]. This suggests that *M. charantia* bioactives may act as fine-tuned modulators of PTPN1 activity rather than simple blockers.

HSP90AA1 serves as a critical chaperone in inflammatory signaling. It is known to be a central mediator of pain-related signaling and neuroinflammation [62]. The present results showed that SG and BSG exhibited robust binding interactions with HSP90AA1 (−9.7 and −9.2 kcal/mol, respectively). Although these affinities were slightly lower than those of the potent inhibitor geldanamycin (−10.6 kcal/mol), they represent substantial target engagement for natural compounds. Conversely, the smaller metabolites (trigonelline, galactonic acid, GABA, isoleucine, leucine, and valine) exhibited weak binding energies ranging from −4.0 to −5.2 kcal/mol, indicating limited direct inhibitory activity against this target.

The nuclear receptor PPARG (or PPARγ) has been identified as a potential therapeutic target for inflammatory diseases [47]. Its activation not only inhibits cytokine production but also promotes the resolution of inflammation via autophagy-mediated suppression of the NLRP3 inflammasome [63]. While synthetic agonists like pioglitazone are effective, our study suggests that *M. charantia* compounds may offer a stronger natural alternative. Docking simulations demonstrated that SG (−9.2 kcal/mol) and BSG (−8.8 kcal/mol) bind to PPARG with greater affinity than pioglitazone (−8.4 kcal/mol). This strong interaction suggests that these bioactives may robustly drive the anti-inflammatory mechanisms essential for treating conditions such as rheumatoid arthritis.

The analysis extended to the the IGF1/IGF1R axis, which has been associated with inflammation [64]. Although IGF1R was not among the 28 common targets identified in network pharmacology, it was included for molecular docking due to its mechanistic role as the receptor for IGF1. The IGF signaling axis is a critical determinant of cell fate, influencing cancer progression [65] and inflammation. Its function is context-dependent: while IGF1 can suppress inflammation in myocardial infarction [66], the activation of IGF1/IGF1R signaling can conversely drive fibrosis and epithelial–mesenchymal transition (EMT) in alveolar cells [67]. Furthermore, inhibiting IGF1R has proven effective in alleviating inflammation in diabetic nephropathy models [68]. In our docking analysis, stigmasterol glucoside (SG) demonstrated superior binding to IGF1R (−10.9 kcal/mol), outperforming the clinical inhibitor linsitinib (−10.7 kcal/mol). However, BSG displayed a lower affinity (−9.7 kcal/mol) compared to the control.

Collectively, these findings position the charantin derivatives (BSG and SG) as the most promising bioactive constituents of *M. charantia*. They exhibited consistently strong affinities across a spectrum of key inflammation-associated proteins, specifically NOS3, EGFR, PTPN1, PPARG, and IGF1R. The quantitative binding affinities derived from the docking simulations are summarized in Table 3, and the detailed intermolecular interactions for the top-performing complexes are visualized in Figure 8.

Interestingly, a comparison of the docking results with the ADMET and Lipinski profiles reveals a correlation between molecular weight/lipophilicity and binding affinity. The larger, more lipophilic steroidal glucosides (BSG and SG) demonstrated significantly higher binding affinities than the smaller, more hydrophilic metabolites (such as GABA and the amino acids). However, as noted in the ADMET analysis, these larger molecules also exhibit lower predicted Caco-2 permeability and potential BBB restrictions, highlighting a common pharmacological trade-off between target binding potency and optimal pharmacokinetic distribution.

Table 3. Binding scores of the selected proteins with their specific control ligands and selected bioactives from *Momordica charantia*. The binding scores which are better than the control ligands are highlighted with bold font.

	Binding score (kcal/mol)					
Proteins	**NOS3**	**HSP90AA1**	**EGFR**	**PTPN1**	**PPARG**	**IGF1R**
Control ligands	L-NIO	Geldanamycin	AG1478	TCS401	Pioglitazone	Linsitinib
	-6.2	-10.6	-8.6	-7.0	-8.4	-10.7
BSG	**-10.5**	-9.2	**-9.1**	**-7.4**	**-8.8**	-9.7
SG	**-10.3**	-9.7	**-10.2**	**-8.5**	**-9.2**	**-10.9**
Trigonelline	**-6.3**	-5.2	-5.6	-5.8	-4.9	-5.4
Galactonic acid	**-6.4**	-5.0	-5.8	-5.6	-4.8	-5.9
GABA	-4.7	-4.0	-4.5	-4.5	-3.9	-3.9
Isoleucine	-5.8	-4.7	-4.9	-5.1	-4.4	-5.0
Leucine	-5.5	-4.9	-5.1	-5.4	-4.4	-4.8
Valine	-5.4	-4.4	-4.6	-4.8	-4.4	-4.7

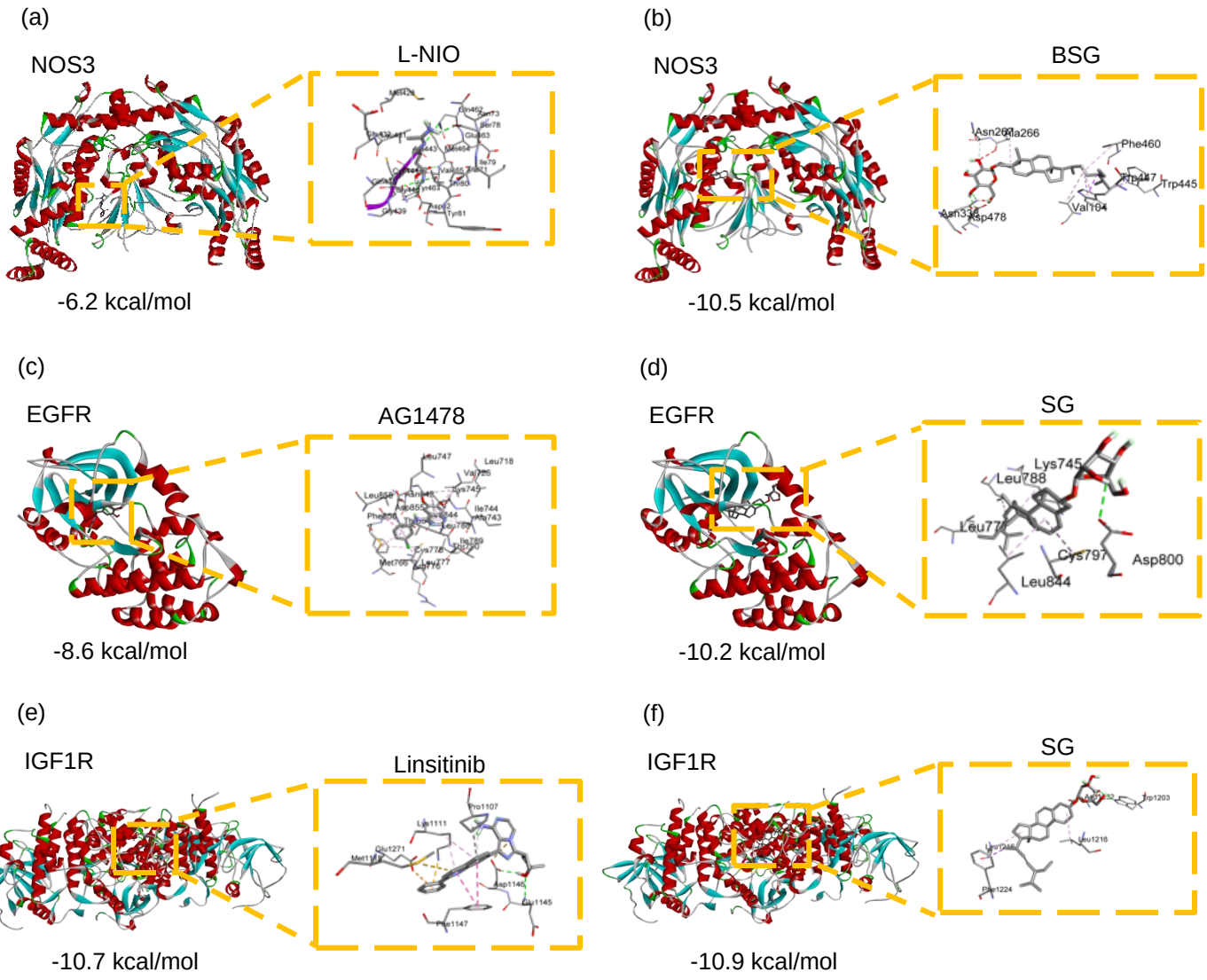


Figure 8. Molecular docking results of *M. charantia* bioactive compounds with inflammation-related targets and their binding scores: (a) NOS3 and L-NIO; (b) NOS3 and BSG; (c) EGFR and AG1478; (d) EGFR and SG; (e) IGF1R and linsitinib; (f) IGF1R and SG. The 3D

and 2D representations of the ligand-protein interactions are provided as Supplementary Figures S3–S5, and the corresponding intermolecular interactions are shown in Supplementary Tables S4–S6.

Conclusions

By delineating the molecular targets of *M. charantia*, this study positions charantin (BSG and SG) as a promising candidate for novel anti-inflammatory drugs. The multi-target profile of the charantin compound addresses the complexity of inflammatory diseases more effectively than single-target agents. Specifically, SG emerged as the lead candidate for receptor modulation, exhibiting exceptional binding affinity for IGF1R and EGFR.

Despite these promising findings, several limitations of this computational approach must be acknowledged. First, molecular docking relies on static *in silico* models; therefore, molecular dynamics (MD) simulations are prioritized for future studies to validate the kinetic and thermodynamic stability of these ligand-receptor complexes over time. Additionally, the network predictions and binding affinities represent a structural hypothesis rather than definitive proof of biological activity. Subsequent *in vitro* and *in vivo* experimental validations, such as cell-based inflammatory assays and specific enzyme inhibition studies, are required to confirm the therapeutic efficacy and pathway modulation proposed in the present study.

Nevertheless, the data strongly supports the repositioning of this traditional remedy as a source of evidence-based phytopharmaceuticals, laying a robust structural foundation for subsequent pre-clinical trials aimed at harnessing plant-based multi-target inhibitors for chronic inflammatory conditions.

Conflicts of Interest

The authors declare that there is no conflict of interest regarding the publication of this paper.

Acknowledgment

KKC is supported by the Malaysian Ministry of Higher Education under Fundamental Research Grant Scheme (FRGS/1/2020/WAB13/UTM/02/1).

References

[1] L. Chen, H. Deng, H. Cui, J. Fang, Z. Zuo, J. Deng, Y. Li, X. Wang, L. Zhao, *Oncotarget* 9 (2017) 7204.
[2] Y. Oishi, I. Manabe, *Int. Immunol.* 30 (2018) 511.
[3] K. R. M. Swamy, *Int. J. Dev. Res.* 13 (2023) 61294.
[4] C. Zhang, M. Huang, R. Hong, H. Chen, *Int. J. Biol. Macromol.* 122 (2019) 619.
[5] G. A. Bhat, H. A. Khan, A. S. Alhomida, P. Sharma, R. Singh, B. A. Paray, *BMC Complement. Altern. Med.* 18 (2018) 162.
[6] S. Y. Lee, W. F. Wong, J. Dong, K. K. Cheng, *Molecules* 25 (2020) 3783.
[7] W. S. Yang, E. Yang, M. J. Kim, D. Jeong, D. H. Yoon, G. H. Sung, K. Y. Lee, J. Y. Cho, *Am. J. Chin. Med.* 46 (2018) 435.
[8] C. Y. Chao, P. J. Sung, W. H. Wang, Y. H. Kuo, *Molecules* 19 (2014) 12777.
[9] C. C. Liaw, H. T. Huang, H. K. Liu, Y. C. Lin, L. J. Zhang, W. C. Wei, S. H. Wang, Y. H. Kuo, Phytochemistry 195 (2022) 113026.
[10] A. Daina, O. Michielin, V. Zoete, *Sci. Rep.* 7 (2017) 42717.
[11] M. Bitew, T. Desalegn, T. B. Demissie, A. Belayneh, M. Endale, R. Eswaramoorthy, *PLoS ONE* 16 (2021) e0260853.
[12] X. Wang, Y. Shen, S. Wang, S. Li, W. Zhang, X. Liu, L. Lai, H. Li, *Nucleic Acids Res.* 45 (2017) W356.
[13] X. Liu, S. Ouyang, B. Yu, Y. Liu, K. Huang, J. Gong, S. Zheng, H. Jiang, *Nucleic Acids Res.* 38 (2010) W609.
[14] L. Yang, H. Li, M. Yang, W. Zhang, M. Li, Y. Xu, H. Zhang, S. Guo, *BioMed Res. Int.* 2020 (2020) 5891016.
[15] A. Daina, O. Michielin, V. Zoete, *Nucleic Acids Res.* 47 (2019) W357.
[16] J. Tong, Y. Ding, D. Zhang, *Medicine* 104 (2025) e43560.
[17] A. Gangwal, I. Ansari, J. A. Sawale, A. Ansari, *In Silico Res. Biomed.* 2 (2026) 100247.
[18] G. M. Basavarajappa, A. Rehman, P. N. Shiroorkar, N. Sreeharsha, M. K. Anwer, B. Aloufi, *Front. Pharmacol.* 14 (2023) 1187079.
[19] G. Stelzer, N. Rosen, I. Plaschkes, S. Zimmerman, M. Twik, S. Fishilevich, T. I. Stein, R. Nudel, I. Lieder, Y.

Mazor, S. Kaplan, D. Dahary, D. Warshawsky, Y. Guan-Golan, A. Kohn, N. Rappaport, M. Safran, D. Lancet, in: *Current Protocols in Bioinformatics*, John Wiley & Sons, Hoboken, NJ, 2016, p. 1.30.1.
[20] J. Piñero, J. M. Ramírez-Anguita, J. Saüch-Pitarch, F. Ronzano, E. Centeno, F. Sanz, L. I. Furlong, *Nucleic Acids Res.* 48 (2020) D845.
[21] J. Piñero, À. Bravo, N. Queralt-Rosinach, A. Gutiérrez-Sacristán, J. Deu-Pons, E. Centeno, J. García-García, L. I. Furlong, *Nucleic Acids Res*. 45 (2017) D833-D839.
[22] Y. Wang, S. H. Yang, K. Zhong, T. Jiang, M. Zhang, H. Y. Kwan, T. Su, *Front. Pharmacol.* 11 (2020) 572387.
[23] S. Batool, M. R. Javed, S. Aslam, F. Noor, H. M. F. Javed, R. Seemab, M. I. Khan, A. Gulnaz, *Pharmaceuticals* 15 (2022) 654.
[24] G. D. Bader, C. W. Hogue, *BMC Bioinformatics* 4 (2003) 2.
[25] Z. Zhai, X. Tao, M. M. Alami, S. Shu, X. Wang, *Curr. Issues Mol. Biol.* 43 (2021) 6.
[26] C. Tao, J. Wang, Z. Gu, H. Ni, Y. Luo, J. Ling, H. Fan, T. Xu, *J. Ethnopharmacol.* 317 (2023) 116695.
[27] S. Huang, F. Mu, F. Li, W. Wang, H. Chen, L. Lei, J. Zhang, J. Wang, *J. Diabetes Res.* 2020 (2020) 7867245.
[28] Y. X. Liu, X. L. Ding, S. Y. Cui, J. J. Liu, G. Ding, *Biomed. Environ. Sci.* 35 (2022) 674.
[29] M. Deodhar, S. B. Al Rihani, M. J. Arwood, L. Darakjian, P. Dow, J. Turgeon, V. Michaud, *Pharmaceutics* 12 (2020) 846.
[30] T. C. Beck, K. R. Beck, J. Morningstar, M. M. Benjamin, R. A. Norris, *Pharmaceuticals* 14 (2021) 472.
[31] J. Warwick, J. Holness, *Semin. Nucl. Med.* 52 (2022) 453.
[32] M. Acosta-Martinez, M. Z. Cabail, *Int. J. Mol. Sci.* 23 (2022) 15330.
[33] Z. Zhang, L. Wang, X. Li, Y. Miao, D. Li, *Int. J. Med. Sci.* 21 (2024) 2837.
[34] X. Gong, D. Xue, H. Meng, B. Xie, L. Zhao, C. Zang, J. Kong, *PLoS ONE* 20 (2025) e0335139.
[35] F. Tang, P. Zhang, W. Zhao, G. Zhu, G. Shen, H. Chen, X. Xu, H. Ren, *Evid.-Based Complement. Altern. Med.* 2022 (2022) 6741995.
[36] H. Liu, H. Lu, X. Fan, S. Chen, X. Chen, W. Gao, *Sci. Rep.* 15 (2025) 12645.
[37] W. Wei, J. X. Yao, T. T. Zhang, J. Y. Wen, Z. Zhang, Y. M. Luo, X. Y. Liu, H. Li, *Front. Neurosci.* 17 (2023) 1059496.
[38] K. Wang, J. Yin, J. Chen, J. Ma, H. Si, D. Xia, *Phytomedicine* 128 (2024) 155258.
[39] S. S. Azam, S. W. Abbasi, *Theor. Biol. Med. Model.* 10 (2013) 63.
[40] F. Ballante, A. J. Kooistra, S. Kampen, C. de Graaf, J. Carlsson, *Pharmacol. Rev.* 73 (2021) 1698.
[41] M. I. Choudhary, M. Shaikh, A. tul-Wahab, A. ur-Rahman, *PLoS ONE* 15 (2020) e0235030.
[42] Y. Gao, S. Zhou, Y. Xu, S. Sheng, S. Y. Qian, X. Huo, *Nitric Oxide* 83 (2019) 33.
[43] X. Ju, X. Yang, T. Yan, H. Chen, Z. Song, Z. Zhang, Z. Lin, Y. Wang, *Clin. Exp. Pharmacol. Physiol.* 46 (2019) 75.
[44] D. Liang, H. Chen, L. Zhao, W. Zhang, J. Hu, Z. Liu, X. Sheng, G. Liang, *Biochim. Biophys. Acta Mol. Basis Dis.* 1864 (2018) 133.
[45] R. Watkins, E. Buckarma, J. Tomlinson, G. Gores, R. Smoot, *HPB* 25 (2023) S53.
[46] S. Jiang, X. Wei, Y. Zhang, L. Wang, L. Wang, M. Wang, J. Sun, H. Zhao, *Biomed. Pharmacother.* 168 (2023) 115640.
[47] R. Kapadia, J. H. Yi, R. Vemuganti, *Front. Biosci.* 13 (2008) 1813.
[48] P. Barata, M. Cooney, A. Tyler, J. Wright, R. Dreicer, J. A. Garcia, *Invest. New Drugs* 36 (2018) 451.
[49] A. Gulbins, M. Horstmann, A. Daser, U. Flögel, M. Oeverhaus, N. E. Bechrakis, A. K. Eckstein, G. E. Görtz, *Front. Endocrinol.* 14 (2023) 1211473.
[50] Y. Fukuyo, C. R. Hunt, N. Horikoshi, *Cancer Lett.* 290 (2010) 24.
[51] R. R. Kitson, D. Kitsonová, D. Siegel, D. Ross, C. J. Moody, *J. Med. Chem.* 67 (2024) 17946.
[52] G. H. Oliveira-Paula, R. Lacchini, J. E. Tanus-Santos, *Gene* 575 (2016) 584.
[53] N. Singh, M. K. Rai, V. Agarwal, V. Agarwal, *Indian J. Rheumatol.* 19 (2024) 100.
[54] A. Pautz, H. Li, H. Kleinert, *Front. Biosci.-Landmark* 26 (2021) 85.
[55] S. N. Villegas, R. Gombos, L. García-López, I. Gutierrez-Perez, J. García-Castillo, D. M. Vallejo, B. Da-Silva, M. Dominguez, *Cell Rep.* 22 (2018) 2541.
[56] S. Cao, Y. Pan, J. Tang, A. S. Terker, J. P. Arroyo Ornelas, G. N. Jin, S. Y. Chen, M. Z. Zhang, *Nat. Commun.* 13 (2022) 4684.
[57] H. D. Londres, J. J. Armada, A. H. Martínez, A. A. Abdo Cuza, Y. H. Sánchez, A. G. Rodríguez, B. E. G. Pérez, T. C. Ramos, *Immunotherapy* 14 (2022) 521.
[58] E. England, D. G. Rees, I. C. Scott, S. Carmen, D. T. Chan, C. E. Chaillan Huntington, R. D. May, E. S. Cohen, *Sci. Rep.* 13 (2023) 9825.
[59] D. Han, D. Lu, S. Huang, J. Pang, Y. Wu, J. Hu, X. Chen, J. Wang, *Redox Biol.* 58 (2022) 102558.
[60] R. Zhao, S. Chen, W. Cui, C. Xie, A. Zhang, L. Yang, H. Dong, *Front. Immunol.* 14 (2023) 1232047.
[61] X. Xu, X. Wang, Y. Guo, Y. Bai, S. He, N. Wang, F. Wang, Y. Yao, *Front. Immunol.* 10 (2019) 1930.
[62] F. Luo, J. Zhang, Y. Miao, D. Wu, H. Shen, M. Lu, *Int. J. Biochem. Cell Biol.* 176 (2024) 106675.
[63] Q. Geng, J. Xu, X. Cao, Z. Wang, Y. Jiao, W. Diao, J. Meng, C. Xiao, *J. Autoimmun.* 146 (2024) 103214.
[64] S. Piñeiro-Hermida, I. P. López, E. Alfaro-Arnedo, R. Torrens, M. Iñiguez, L. Alvarez-Erviti, J. A. Esteban, J. G. Pichel, *Sci. Rep.* 7 (2017) 4290.
[65] P. Wang, V. C. Mak, L. W. Cheung, *Genes Dis.* 10 (2023) 199.
[66] R. Nederlof, S. Reidel, A. Spychala, S. Gödecke, A. Heinen, T. Lautwein, J. W. Fischer, A. Gödecke, *Front. Immunol.* 13 (2022) 908023.
[67] Y. Zhang, J. Liang, N. Cao, J. Gao, L. Song, X. Tang, *Cell Death Discov.* 8 (2022) 500.
[68] J. Li, R. Dong, J. Yu, S. Yi, J. Da, F. Yu, Y. Zha, *Drug Des. Devel. Ther.* 12 (2018) 2887.